

Received July 30, 2019, accepted August 12, 2019, date of publication August 20, 2019, date of current version September 12, 2019.

Digital Object Identifier 10.1109/ACCESS.2019.2936458

# A Compact-Size Wideband Optically-Transparent Water Patch Antenna Incorporating an Annular Water Ring

JIE SUN<sup>1</sup>, (Student Member, IEEE), AND KWAI-MAN LUK<sup>1,2</sup>, (Fellow, IEEE)

<sup>1</sup>Department of Electrical Engineering, City University of Hong Kong, Hong Kong

<sup>2</sup>State Key Laboratory of Terahertz and Millimeter Wave, City University of Hong Kong, Hong Kong

Corresponding author: Jie Sun (sunjie1106@gmail.com)

This work was supported by the Research Grant Council of Hong Kong, Hong Kong, under Project 7004844 (CityU 11214517) and Project 9042377 (CityU 11277116).

**ABSTRACT** A wideband optically-transparent water patch antenna with a compact size is proposed. Both the water patch and the water ground plane are made of distilled water to realize the highly optical transparency. Particularly, by simply incorporating an annular water ring under the water patch, the center frequency can be reduced from 2.3 GHz to 1.95 GHz, while the corresponding size of the water patch can be reduced by 28%. Both the simulation and the measurement are carried out for verification. The measured results turn out that a wide impedance bandwidth of 41.8% with  $SWR < 2$ , the maximum gain of 1.56 dBi, radiation efficiency up to 78% and stable monopolar radiation pattern with linear polarization can be achieved. Additional, the effects of the annular water ring on the antenna performance are analyzed and discussed.

**INDEX TERMS** Water patch antenna, transparent antenna, compact size, monopolar radiation pattern, annular water ring.

## I. INTRODUCTION

Antennas with novel materials have attracted more interests in research institutions and technical companies. Various novel materials are utilized, including textiles, plasmonic and fabric substrates, liquid metals, glass, ethyl acetate [1]–[9]. Among all these materials, water becomes popular for its unique merits, such as low in material cost, easy access, liquid and flexible configuration, highly optical transparency [10]. Generally, water can be divided into two categories. One is salt water or sea water and another one is distilled water or pure water. Distilled water can be viewed as a pure dielectric substrate with high dielectric constant at microwave frequencies, which could be utilized to design dielectric resonator antennas (DRA) [11], [12]. Salt water can serve as a conductor since it has some degree of conductivity to support the current flowing inside. Thus, salt water is often utilized to form monopole or loop antennas, especially for maritime environments [13]–[15].

Dense dielectric patch antenna (DDPA) was proposed in 2013 [16]. Based on the basic patch antenna concept

with the top metallic patch replaced with a thin dielectric substrate of relative high dielectric constant, the DDPA was achieved with similar performance as the conventionally metallic patch antenna. For millimeter-wave applications, the DDPA shows better characteristics in efficiency over metallic patch antennas since the caused conductor loss can be reduced [17]. Regarding the application at microwave frequencies, the DDPA can be applied to construct patch antennas composed of novel materials to address various challenges of sophisticated wireless communications in the future. Basically, water is a kind of material with relative high permittivity of about 80 at microwave frequencies at room temperature [18]. Therefore, water can be regarded as one of the liquid dense dielectric substrate for realizing the DDPA. The first patch antenna using distilled water was proposed in 2015 with the top metallic patch replaced by a pure water layer [19]. The working principle and results in [19] had demonstrated the successful realization of the concept of the water patch antenna. Following the prototype in [19], a transparent water patch antenna with both the patch and the ground plane made of distilled water was reported [20]. The obtained performance in [20] shows that the patch mode can be primarily excited and resonant in the middle substrate

The associate editor coordinating the review of this article and approving it for publication was Chan Hwang See.

between the water patch and the water ground plane, resulting in the same working principle as the metallic patch antenna.

For a patch antenna with monopolar radiation pattern, the patch diameter is about one wavelength at its resonant frequency, which is physically larger and undesirable for many practical applications [21]–[30]. By etching slots on the patch or employing the folded patch, the total current length along the patch can be extended. Thus, a lower operating frequency and a compact patch size in terms of wavelength are achieved [31]–[34]. However, since no current exists inside distilled water, these approaches will not effectively work for water patch antennas. Incorporating a shorting pin close to the feeding probe is another simply approach to reduce the patch size due to the strong capacitive coupling effect between the shorting pin and the feeding probe [35]–[37]. However, this method will introduce additional metallic portions, decreasing the total optical transparency for the water patch antenna.

In this paper, a compact-size optically-transparent water patch antenna is proposed by simply incorporating an annular water ring under the water patch. It shows that with an annular water ring, the center frequency can be reduced from 2.3 GHz to 1.95 GHz, and the corresponding size of the water patch can decrease by 28%. Both the patch and the ground plane are made of distilled water to obtain the highly optical transparency. A wide impedance bandwidth of 41.8% with stable monopolar radiation pattern over the entire frequencies can be experimentally achieved.

II. ANTENNA CONFIGURATION

The proposed antenna configuration is shown in Fig. 1, with detailed dimensions given in Table. 1. The fabricated prototype is given in Fig. 2. The compact water patch antenna consists of four main portions: a water patch layer, a water ground plane layer, an annular water ring and a disk-loaded metallic probe. All the utilized water in the proposed configuration is distilled water, which is a kind of low-cost and optically transparent material. Both the water patch and the water ground plane are in circular shape for obtaining an omnidirectional radiation pattern. A disk-loaded probe is employed in the center position to capacitively excite the antenna. The probe connects to a coaxial cable of 50 ohm impedance. The thickness of the disk is 1.0 mm. The inner conductor of the coaxial cable acts as the vertical portion of the disk-loaded probe. In order to ensure the EM waves can be effectively transmitted into the middle substrate (plexiglass), the coaxial cable is arranged to entirely penetrate through the water ground plane into the middle substrate. The entire configuration is enclosed by a transparent container comprising the plexiglass. Particularly, a cylindrical hollow air cavity is left in the middle substrate for placing the disk-loaded probe. The measured dielectric constant and the dielectric loss tangent of the used plexiglass at room temperature are shown in Fig. 3. The measured dielectric constant and dielectric loss tangent of used distilled water had been carried out with results shown in [20]. For enhancing the accuracy, both the frequency-varying value of the dielectric

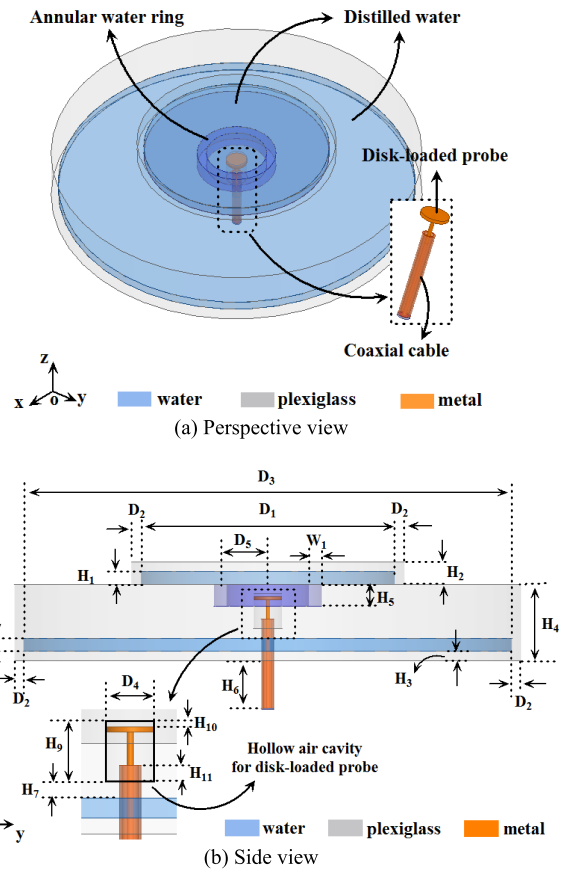


FIGURE 1. Configuration of the proposed compact-size water patch antenna: (a) Perspective view, (b) Side view.

TABLE 1. Dimension of the proposed compact-size water patch antenna.

Parameter	H <sub>1</sub>	H <sub>2</sub>	H <sub>3</sub>	H <sub>4</sub>	H <sub>5</sub>
Value (mm)	4	7	3	23.5	7
Parameter	H <sub>6</sub>	H <sub>7</sub>	H <sub>8</sub>	H <sub>9</sub>	H <sub>10</sub>
Value (mm)	20.5	3	3.5	11	1
Parameter	H <sub>11</sub>	D <sub>1</sub>	D <sub>2</sub>	D <sub>3</sub>	D <sub>4</sub>
Value (mm)	3	80	3	154	9
Parameter	D <sub>5</sub>	W <sub>1</sub>			
Value (mm)	15	4			

constant and dielectric loss tangent of distilled water and plexiglass have been considered in the simulation process. All the used value of plexiglass and distilled water in the simulation are in the case of room temperature of approximately 20 °C in accordance with the practical experimental condition. The size of the water patch and the water ground plane is 0.52 λ<sub>0</sub> × 0.52 λ<sub>0</sub> and 1.0 λ<sub>0</sub> × 1.0 λ<sub>0</sub> respectively. The thickness of middle substrate is 0.11 λ<sub>0</sub> (λ<sub>0</sub> refers to one wavelength in air at the center frequency of 1.95 GHz).

III. ANTENNA WORKING PRINCIPLE

A. ELECTRIC FIELD DISTRIBUTION

Because almost no current exist inside distilled water, only the distributions of electric field are studied in order to

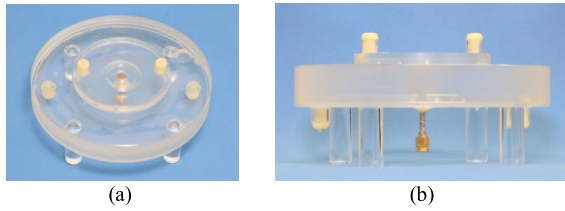


FIGURE 2. Prototype of the proposed compact-size water patch antenna: (a) Perspective view, (b) Side view.

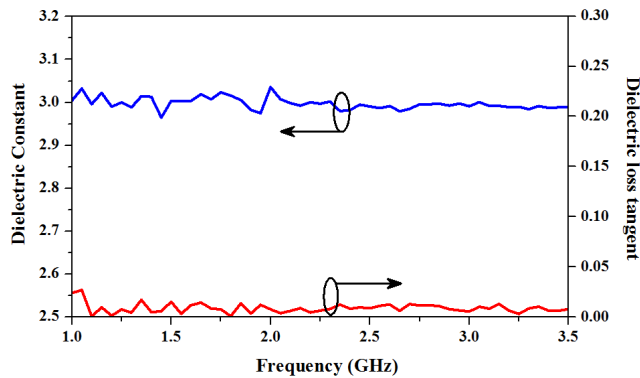


FIGURE 3. Measured dielectric constant and dielectric loss tangent of the plexiglass at room temperature used in the proposed compact-size water patch antenna.

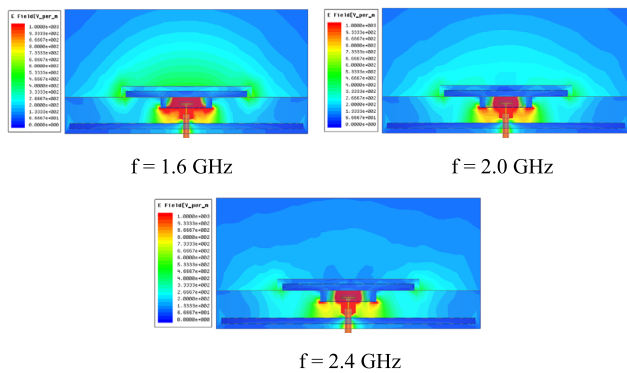


FIGURE 4. Simulated magnitude distributions of the electric field in the E-plane of the proposed compact-size water patch antenna across the entire frequencies.

investigate the working principle, and the performance is shown in Fig. 4 and Fig. 5.

The magnitude distributions of electric field in the E-plane are shown in Fig. 4. The majority of electric fields are confined between the water patch and the water ground plane, with very few electromagnetic (EM) waves inside distilled water. This is due to the higher dielectric constant of distilled water ( $\sim 80$ ) and lower dielectric constant of plexiglass ( $\sim 3$ ) at room temperature, leading to an internal reflection for most excited EM waves in the middle substrate on the boundary surface of water. Thus, the DRA mode of water will be reduced. The EM waves mainly resonant in the middle substrate of plexiglass, and then radiate into the free space through an annular open slot at the edge of the water patch.

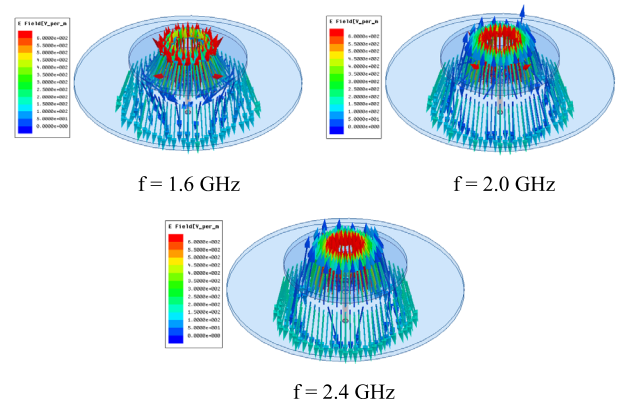


FIGURE 5. Simulated direction distributions of the electric field in the middle substrate of the proposed compact-size water patch antenna across the entire frequencies.

The direction distributions of electric field in the middle substrate of plexiglass are illustrated in Fig. 5. In order to generate a monopolar radiation pattern for a patch antenna, the  $TM_{02}$  mode needs to be excited. The electric field distributions of the  $TM_{02}$  mode for a patch antenna shows a sinusoidal distribution of one wavelength with the maximum electric field occurs at center and edge positions [22]. As seen from Fig. 5, the electric field distributions in the proposed water patch antenna is the same as in the metallic patch antenna operating at  $TM_{02}$  mode, demonstrating that the patch mode is primarily excited.

### B. FREQUENCY DECREASE BY ANNULAR WATER RING

By simply incorporating an annular water ring in the middle substrate with the patch size unchanged, the center frequency can be reduced from 2.3 GHz to 1.95 GHz. As shown in Fig. 4 and Fig. 5, distilled water actually provides a kind of boundary with almost the same function of perfect electric conductor (PEC) to confine the EM waves. Besides, as the antenna radiation is from the circle edge of the water patch, the water patch along with the water ground plane can be actually regarded as a kind of transmission line to guide the propagation of excited EM waves in the middle substrate (plexiglass). Thus, the performance of frequency decrease of the water patch antenna can also be characterized using the transmission line theory.

Usually, the patch antenna with monopolar radiation pattern can be modelled as a transmission line with one wavelength in length at its resonant frequency. As shown in Fig. 6, the EM waves propagate along the transmission line consists of the water patch and the water ground plane, and then radiate at the edge of the water patch. The edge serves as an open slot of the transmission line, which can be modelled as a parallel circuit composed of shunt capacitance  $C$  and shunt conductance  $G$ . The water patch can be modelled as a section of transmission line of characteristic impedance  $Z_{\text{water}}$ . The disk-loaded probe gives the input excitation in the center position. When incorporating an annular water ring under the water patch, the characteristic impedance of

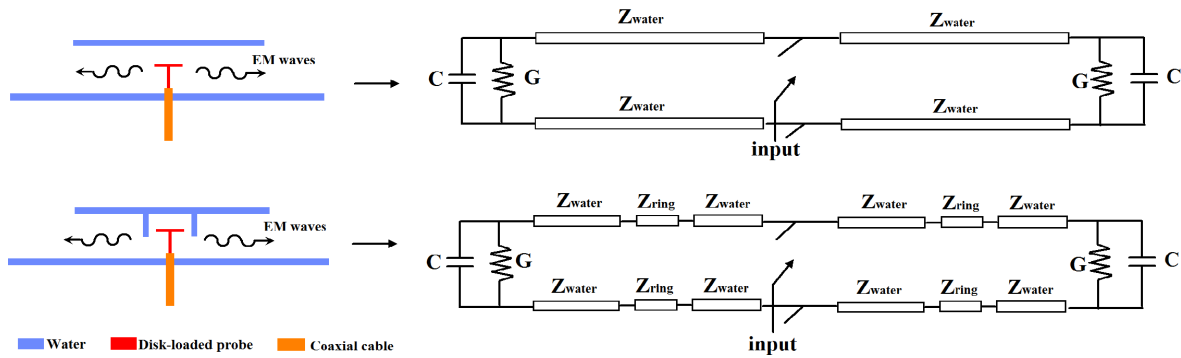


FIGURE 6. Equivalent circuit of the cross-section view of the proposed water patch antenna without and with an annular water ring.

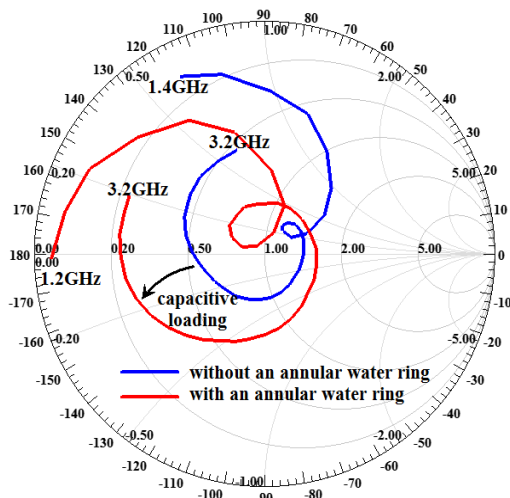


FIGURE 7. Comparison of the input impedance variation on smith chart for the proposed water patch antenna with and without an annular water ring.

the transmission line with water ring changes into  $Z_{ring}$ , resulting in the variation of total input impedance. Incorporating an annular water ring will decrease the gap distance between the water patch layer and the water ground plane layer, leading to an increased shunt capacitive  $C$ . Thus,  $Z_{ring}$  actually shows more capacitive than  $Z_{water}$ , which is equivalent to the capacitive coupling to the original equivalent circuit of water patch. The locus of input impedance on smith chart for the proposed water patch antenna have been shown in Fig. 7. It shows that by incorporating an annular water ring, the locus has a counter-clockwise shift, demonstrating the effect of capacitive coupling. At the frequencies below the resonance of the water patch antenna, the inductive reactance of the input impedance can be compensated by the capacitive coupling of the water ring, resulting in a lower operating bandwidth.

IV. PERFORMANCE AND DISCUSSION

Both the simulation and the measurement have been carried out for verification. The S-parameter was measured by Agilent E5071C network analyzer and the radiation pattern, gain and efficiency were measured by SATIMO complex antenna measurement system.

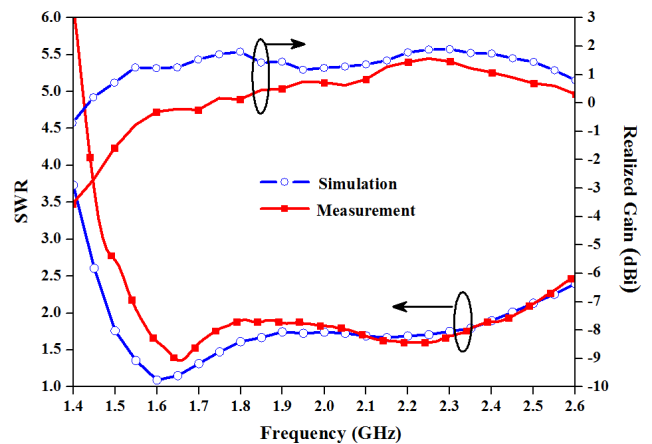


FIGURE 8. Simulated and measured SWRs and realized gains for the proposed compact water patch antenna.

A. BANDWIDTH AND GAIN

The simulated and measured results of SWR and gain are illustrated in Fig. 8. The measured and simulated impedance bandwidth with  $SWR < 2$  is 41.8% (from 1.57 to 2.4 GHz) and 46.2% (from 1.5 to 2.4 GHz), respectively. The simulated gain varies from 0.7 to 1.8 dBi, and the measured gain ranges between  $-0.3$  and 1.56 dBi. The difference between the simulated and measured gain is due to the inevitable measurement system error and fabrication error. Also, some possible air bubbles existing inside distilled water will cause some uncertainty deviations. The gain is not as high as in the metallic patch due to the dielectric loss of distilled water and a smaller size of the water ground plane.

B. RADIATION PATTERN

The simulated and measured radiation pattern over the entire bandwidth is shown in Fig. 9. The monopolar radiation pattern is achieved with the small cross-polarization and a wide beamwidth. In the E-plane, the conical beam radiation pattern is obviously obtained. The direction of the maximum radiation intensity occur at elevation angle of around 78 degree. The omnidirectional radiation pattern in the H-plane is achieved with quite small cross-polarization of less than  $-20$  dB.

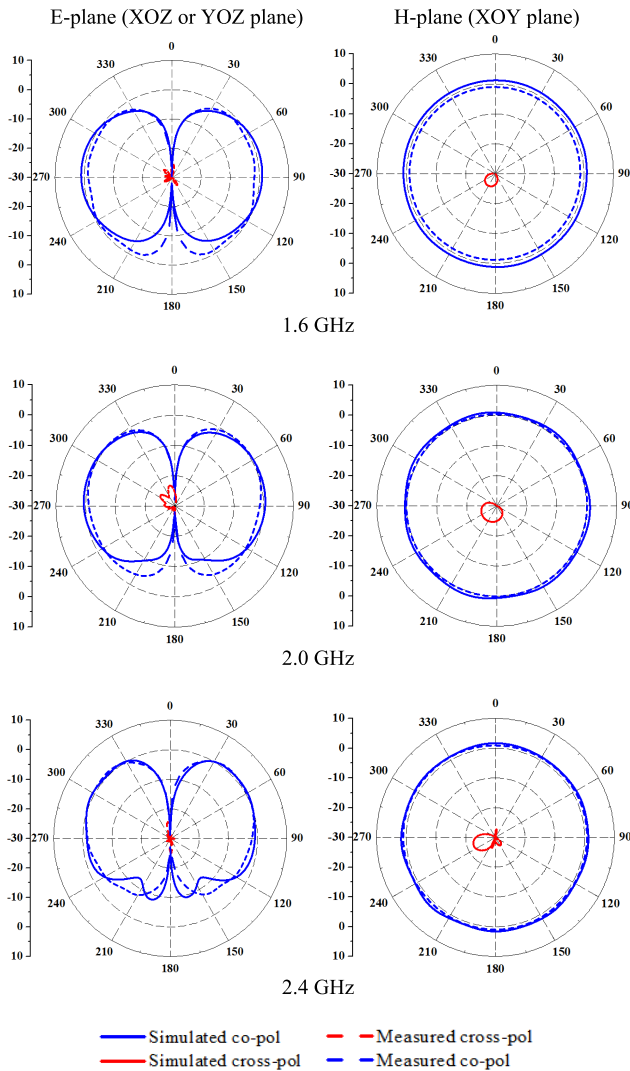


**FIGURE 9.** Simulated and measured radiation pattern in the E-planes (elevation planes) and H-planes (azimuth planes) across the operating bandwidth.

**C. EFFICIENCY**

The simulated and measured radiation efficiency are shown in Fig. 10. The simulated radiation efficiency ranges from 80% to 90%, while the measured radiation efficiency varies between 70% and 78%. The difference between them is mainly caused by the fabrication tolerance and some possible tiny air bubbles inside distilled water, causing deviation of distilled water volume between the simulation and the measurement. Since the most EM waves resonant in the middle substrate with lower dielectric loss rather than being absorbed by distilled water, good efficiency can be obtained accordingly.

**D. DISCUSSION ON ANNULAR WATER RING**

The annular water ring is the crucial portion to the size reduction and overall bandwidth because it can significantly affect the input impedance. Therefore, the height ( $H_5$ ) and width ( $W_1$ ) of the annular water ring are studied and analyzed.

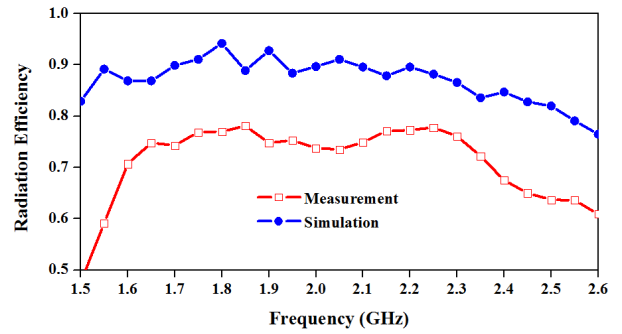


**FIGURE 10.** Simulated and measured radiation efficiencies for the proposed compact-size water patch antenna.

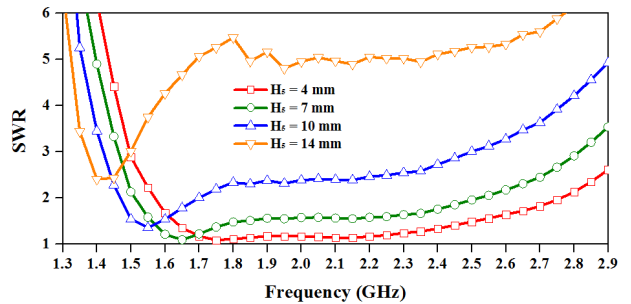


**FIGURE 11.** Simulated SWRs for the proposed compact-size water patch antenna with different height of the annular water ring ( $H_5$ ).

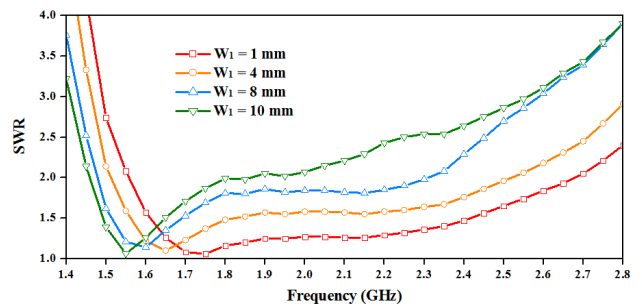


**FIGURE 12.** Simulated SWRs for the proposed compact-size water patch antenna with different widths of the annular water ring ( $W_1$ ).

The results of SWR versus  $H_5$  and  $W_1$  have been shown in Fig. 11 and Fig. 12. It shows that increased  $H_5$  and  $W_1$  can result in the lower operating frequencies. This is mainly because a larger  $H_5$  or  $W_1$  will cause increased effect of capacitive coupling on the equivalent circuit of original water patch since the gap between the water ring and the water ground plane becomes smaller or longer. Besides, the change of  $H_5$  and  $W_1$  will result in obvious variation of bandwidth due to its capacitive coupling effect on the input impedance. However, a wide bandwidth can still be achieved by choosing suitable dimensions of the disk-loaded metallic probe.

A comparison between water patch antennas with and without an annular water ring is depicted in Fig. 13 and Table. 2. The dimensions of the disk and height of middle substrate are properly chosen for achieving the wideband characteristic. By adding an annular water ring, both the real

**TABLE 2.** Comparison of simulated results between water patch antennas with and without an annular water ring.

	Center Frequency	Diameter of water patch	Diameter of water ground plane	Imp. BW% (SWR < 2)
Water patch antenna without an annular water ring	2.3 GHz	80 mm (1.05 λ <sub>g</sub> )	154 mm (2.01 λ <sub>g</sub> )	52% (1.72 – 2.9 GHz)
Water patch antenna with an annular water ring	1.95 GHz	80 mm (0.89 λ <sub>g</sub> )	154 mm (1.71 λ <sub>g</sub> )	46.2% (1.5 - 2.4 GHz)

λ<sub>g</sub> refers to the wavelength in terms of the middle substrate at center frequency in their respective passbands. Imp. BW% refers to the impedance bandwidth in the simulation.

**TABLE 3.** Comparison of various monopolar patch antennas.

	Material of patch	Substrate dielectric constant	Polarization	Center frequency (GHz)	Diameter of circular patch	Substrate thickness	Imp. BW% ( S <sub>11</sub>   < -10 dB or SWR < 2)	Max. Gain (dBi or dBic)
[21]	Metal	2.55	LP	5.2	1.17 λ	0.04 λ	3.3%	4.2
[22]	Metal	2.33	LP	2.26	1.1 λ	0.037 λ	18%	6.0
[23]	Metal	2.65	LP	5.76	2.03 λ	0.047 λ	27.4%	6.0
[24]	Metal	1.0	LP	2.15	1.0 λ	0.172 λ	52%	5.0
[25]	Metal	1.0	LP	1.91	0.955 λ	0.13 λ	30%	6.5
[26]	Metal	2.94	LP	6.05	2.14 λ	0.05 λ	12.8%	5.7
[27]	Metal	2.94	CP	5.7	0.98 λ	0.1 λ	28%	4.9
[28]	Metal	2.33	LP	1.88	1.45 λ	0.06 λ	25.5%	5.9
[29]	Metal	2.2	CP	2.45	1.14 λ	0.042 λ	16.6%	1.1
[30]	Metal	1.0	LP	2.55	1.054 λ	0.051 λ	23.5%	6.9
<b>This work</b>	Water	3.0	LP	1.95	0.89 λ	0.19 λ	42%	1.56

λ refers to the wavelength of center frequency in the middle substrate for respective antennas. Imp. BW% refers to the impedance bandwidth.

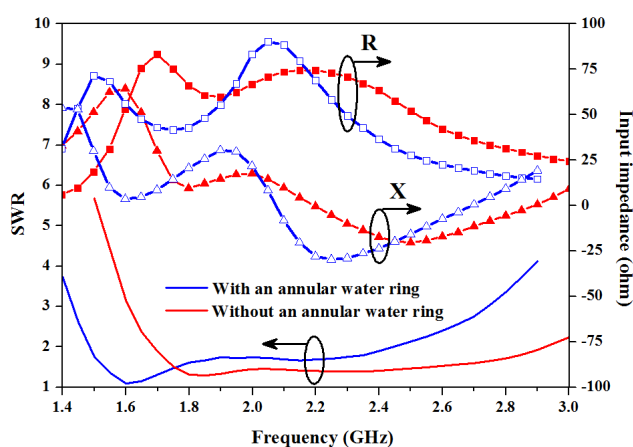


**FIGURE 13.** Simulated SWRs and input impedances for the water patch antennas with or without annular water ring.

and imaginary part of input impedance shift to lower frequencies with the center frequency decreasing to 1.95 GHz from 2.3 GHz. The corresponding size of the water patch is reduced by 28%. This is because the input reactance is inductive

below 1.8 GHz for the water patch antenna without an annular water ring, as shown in Fig. 13. By incorporating an annular water ring, the capacitive effect of the annular water ring can significantly compensate a great number of inductive input reactance below 1.8 GHz, resulting in a resonance (zero crossing of input reactance) occurring at a lower frequency below 1.8 GHz. Thus, the center frequency is reduced and the size of water patch in terms of wavelength of center frequency is miniaturized.

**E. COMPARISON AND DISCUSSION**

A comparison of various reported monopolar patch antennas is illustrated in Table. 3. It shows that a thicker substrate or a lower dielectric constant of substrate can result in a wider bandwidth, as provided in [24] and [25]. In [23] and [26], an additional coupled annular ring was added to enhance the bandwidth so that their patch size are large. When comparing with the monopolar patch antennas composed of metal, the water patch antenna can also achieve a wide impedance bandwidth of over 40% if a thick substrate is used. The realized gain is up to 1.56 dBi, which is lower than most reported

monopolar metallic patch antennas due to the dielectric loss of distilled water at the operating frequencies.

## V. CONCLUSION

A compact-size optically transparent water patch antenna is demonstrated in this paper. By simply incorporating an annular water ring under the water patch, the center frequency can be reduced from 2.3 GHz to 1.95 GHz, and the size of the water patch can be reduced by 28%. A disk-loaded probe is employed in the center position to excite the water patch antenna and also enhance the bandwidth. The water patch, the water ground plane and an annular water ring are all composed of distilled water, which is low material cost, easily available and 100% optically transparent. The entire compact water patch antenna is enclosed by the transparent plexiglass. The results turn out that a wide impedance bandwidth of 41.8% (from 1.57 to 2.4 GHz with  $SWR < 2$ ), the maximum gain of 1.56 dBi, radiation efficiency up to 78%, and stable monopolar radiation pattern can be achieved.

## ACKNOWLEDGMENT

The authors would like to thank Mr. Chun Kwong LAU for his earnest assistance in the antenna fabrication.

## REFERENCES

- [1] K. Li, D. Liu, C.-C. Ho, F. Lu, and A. Xu, "Compact ultrabroadband plasmonic antenna: Potential applications in logic binary encoding," *IEEE Photon. Technol. Lett.*, vol. 27, no. 3, pp. 268–271, Feb. 1, 2015.
- [2] T. F. Kennedy, P. W. Fink, A. W. Chu, N. J. Champagne, G. Y. Lin, and M. A. Khayat, "Body-worn E-textile antennas: The good, the low-mass, and the conformal," *IEEE Trans. Antennas Propag.*, vol. 57, no. 4, pp. 910–918, Apr. 2009.
- [3] R. Moro, S. Agneessens, H. Rogier, and M. Bozzi, "Wearable textile antenna in substrate integrated waveguide technology," *Electron. Lett.*, vol. 48, no. 16, pp. 985–987, Aug. 2012.
- [4] S. Sankaralingam and B. Gupta, "Determination of dielectric constant of fabric materials and their use as substrates for design and development of antennas for wearable applications," *IEEE Trans. Antennas Propag.*, vol. 59, no. 12, pp. 3122–3130, Dec. 2010.
- [5] D. Rodrigo, L. Jofre, and B. A. Cetiner, "Circular beam-steering reconfigurable antenna with liquid metal parasitics," *IEEE Trans. Antennas Propag.*, vol. 60, no. 4, pp. 1796–1802, Apr. 2012.
- [6] K. W. Leung, Y. M. Pan, X. S. Fang, E. H. Lim, K.-M. Luk, and H. P. Chan, "Dual-function radiating glass for antennas and light covers—Part I: Omnidirectional glass dielectric resonator antennas," *IEEE Trans. Antennas Propag.*, vol. 61, no. 2, pp. 578–586, Feb. 2013.
- [7] K. W. Leung, X. S. Fang, Y. M. Pan, E. H. Lim, K. M. Luk, and H. P. Chan, "Dual-Function radiating glass for antennas and light covers—Part II: Dual-band glass dielectric resonator antennas," *IEEE Trans. Antennas Propag.*, vol. 61, no. 2, pp. 587–597, Feb. 2013.
- [8] Z. Chen and H. Wong, "Wideband glass and liquid cylindrical dielectric resonator antenna for pattern reconfigurable design," *IEEE Trans. Antennas Propag.*, vol. 65, no. 5, pp. 2157–2164, May 2017.
- [9] Z. Chen, H. Wong, and J. Kelly, "A polarization-reconfigurable glass dielectric resonator antenna using liquid metal," *IEEE Trans. Antennas Propag.*, vol. 67, no. 5, pp. 3427–3432, May 2019.
- [10] L. Xing, Y. Huang, Y. Shen, S. Al Ja'afreh, Q. Xu, and R. Alrawashdeh, "Further investigation on water antennas," *IET Microw., Antennas Propag.*, vol. 9, no. 8, pp. 735–741, May 2015.
- [11] Y.-H. Qian and Q.-X. Chu, "A broadband hybrid monopole-dielectric resonator water antenna," *IEEE Antennas Wireless Propag. Lett.*, vol. 16, pp. 360–363, 2016.
- [12] R. Zhou, H. Zhang, and H. Xin, "Liquid-based dielectric resonator antenna and its application for measuring liquid real permittivities," *IET Microw., Antennas Propag.*, vol. 8, no. 4, pp. 255–262, Mar. 2014.
- [13] C. Hua, Z. Shen, and J. Lu, "High-efficiency sea-water monopole antenna for maritime wireless communications," *IEEE Trans. Antennas Propag.*, vol. 62, no. 12, pp. 5968–5973, Dec. 2014.
- [14] C. Hua and Z. Shen, "Shunt-excited sea-water monopole antenna of high efficiency," *IEEE Trans. Antennas Propag.*, vol. 63, no. 11, pp. 5185–5190, Sep. 2015.
- [15] M. Wang and Q.-X. Chu, "High-efficiency and wideband coaxial dual-tube hybrid monopole water antenna," *IEEE Antennas Wireless Propag. Lett.*, vol. 17, pp. 799–802, 2018.
- [16] H. W. Lai, K.-M. Luk, and K. W. Leung, "Dense dielectric patch antenna—A new kind of low-profile antenna element for wireless communications," *IEEE Trans. Antennas Propag.*, vol. 61, no. 8, pp. 4239–4245, Aug. 2013.
- [17] Y. Li and K.-M. Luk, "Wideband perforated dense dielectric patch antenna array for millimeter-wave applications," *IEEE Trans. Antennas Propag.*, vol. 63, no. 8, pp. 3780–3786, Aug. 2015.
- [18] T. Meissner and F. J. Wentz, "The complex dielectric constant of pure and sea water from microwave satellite observations," *IEEE Trans. Geosci. Remote Sens.*, vol. 42, no. 9, pp. 1836–1849, Sep. 2004.
- [19] Y. Li and K.-M. Luk, "A water dense dielectric patch antenna," *IEEE Access*, vol. 3, pp. 274–280, 2015.
- [20] J. Sun and K.-M. Luk, "A wideband low cost and optically transparent water patch antenna with omnidirectional conical beam radiation patterns," *IEEE Trans. Antennas Propag.*, vol. 65, no. 9, pp. 4478–4485, Sep. 2017.
- [21] Y. J. Guo, A. Paez, R. A. Sadeghzadeh, and S. K. Barton, "A circular patch antenna for radio LAN's," *IEEE Trans. Antennas Propag.*, vol. 45, no. 1, pp. 177–178, Jan. 1997.
- [22] J. Liu, Q. Xue, H. Wong, H. W. Lai, and Y. Long, "Design and analysis of a low-profile and broadband microstrip monopolar patch antenna," *IEEE Trans. Antennas Propag.*, vol. 61, no. 1, pp. 11–18, Jan. 2013.
- [23] J. Liu, S. Zheng, Y. Li, and Y. Long, "Broadband monopolar microstrip patch antenna with shorting vias and coupled ring," *IEEE Antennas Wireless Propag. Lett.*, vol. 13, pp. 39–42, 2013.
- [24] K. W. Chan, K. F. Tong, and K. M. Luk, "Wideband circular patch antenna operated at  $TM_{01}$  mode," *Electron. Lett.*, vol. 35, no. 24, pp. 2070–2071, Nov. 1999.
- [25] Y.-X. Guo, M. Y. W. Chia, Z. N. Chen, and K.-M. Luk, "Wide-band L-probe fed circular patch antenna for conical-pattern radiation," *IEEE Trans. Antennas Propag.*, vol. 52, no. 4, pp. 1115–1116, Apr. 2004.
- [26] A. Al-Zoubi, F. Yang, and A. Kishk, "A broadband center-fed circular patch-ring antenna with a monopole like radiation pattern," *IEEE Trans. Antennas Propag.*, vol. 57, no. 3, pp. 789–792, Mar. 2009.
- [27] W. Lin and H. Wong, "Circularly polarized conical-beam antenna with wide bandwidth and low profile," *IEEE Trans. Antennas Propag.*, vol. 62, no. 12, pp. 5974–5982, Dec. 2014.
- [28] L. Ge and K.-M. Luk, "Frequency-reconfigurable low-profile circular monopolar patch antenna," *IEEE Trans. Antennas Propag.*, vol. 62, no. 7, pp. 3443–3449, Jul. 2014.
- [29] Y. Shi and J. Liu, "Wideband and low-profile omnidirectional circularly polarized antenna with slits and shorting-vias," *IEEE Antennas Wireless Propag. Lett.*, vol. 15, pp. 686–689, 2016.
- [30] W. Lin, H. Wong, and R. W. Ziolkowski, "Wideband pattern-reconfigurable antenna with switchable broadside and conical beams," *IEEE Antennas Wireless Propag. Lett.*, vol. 16, pp. 2638–2641, 2017.
- [31] K. M. Luk, R. Chair, and K. F. Lee, "Small rectangular patch antenna," *Electron. Lett.*, vol. 34, no. 25, pp. 2366–2367, Dec. 1998.
- [32] K.-F. Lee and K.-F. Tong, "Microstrip patch antennas—Basic characteristics and some recent advances," *Proc. IEEE*, vol. 100, no. 7, pp. 2169–2180, Jul. 2012.
- [33] H. Iwasaki, "A circularly polarized small-size microstrip antenna with a cross slot," *IEEE Trans. Antennas Propag.*, vol. 44, no. 10, pp. 1399–1401, Oct. 1996.
- [34] J.-H. Lu, C.-L. Tang, and K.-L. Wong, "Single-feed slotted equilateral-triangular microstrip antenna for circular polarization," *IEEE Trans. Antennas Propag.*, vol. 47, no. 7, pp. 1174–1178, Jul. 1999.
- [35] R. B. Waterhouse and S. D. Targonski, "Performance of microstrip patches incorporating a single shorting post," in *Proc. IEEE Antennas Propag. Soc. Int. Symp.*, Baltimore, MD, USA, Jul. 1996, pp. 29–32.
- [36] R. B. Waterhouse, S. D. Targonski, and D. M. Kokotoff, "Improving the mechanical tolerances and radiation performance of shorted patches," in *Proc. IEEE Antennas Propag. Soc. Int. Symp.*, Montreal, QC, Canada, Jul. 1996, pp. 1852–1855.
- [37] R. B. Waterhouse, S. D. Targonski, and D. M. Kokotoff, "Design and performance of small printed antennas," *IEEE Trans. Antennas Propag.*, vol. 46, no. 11, pp. 1629–1633, Nov. 1998.



**JIE SUN** (S'15) was born in Nanjing, Jiangsu, China. He received the B.S. degree from the Nanjing University of Science and Technology, Nanjing, China, in 2014. He is currently pursuing the Ph.D. degree in electronic engineering with the City University of Hong Kong, Hong Kong.

His current research interests include water patch antennas, liquid antennas, dense dielectric patch antennas, transparent antennas, and millimeter-wave antennas. He was a recipient of

Best Student Paper Award in the 2017 IEEE International Workshop on Electromagnetics: Applications and Student Innovation Competition, held at University College London (UCL), London, U.K.



**KWAI-MAN LUK** (M'79–SM'94–F'03) received the B.Sc. (Eng.) and Ph.D. degrees in electrical engineering from The University of Hong Kong, in 1981 and 1985, respectively.

He joined the Department of Electronic Engineering, City University of Hong Kong, in 1985, as a Lecturer. Two years later, he moved to the Department of Electronic Engineering, The Chinese University of Hong Kong, where he spent four years. In 1992, he returned to the City University of Hong Kong, where he served as the Head of Department of Electronic Engineering from 2004 to 2010 and the Director of State Key Laboratory of Millimeter Waves from 2008 to 2013, and is currently the Chair Professor of electronic engineering. He is the author of 4 books, 11 research book chapters, over 360 journal papers, and 250 conference papers. His recent research interests include design of patch antennas, magneto-electric dipole antennas, dense dielectric patch antennas, and open resonator antennas for various wireless applications.

of Hong Kong, where he served as the Head of Department of Electronic Engineering from 2004 to 2010 and the Director of State Key Laboratory of Millimeter Waves from 2008 to 2013, and is currently the Chair Professor of electronic engineering. He is the author of 4 books, 11 research book chapters, over 360 journal papers, and 250 conference papers. His recent research interests include design of patch antennas, magneto-electric dipole antennas, dense dielectric patch antennas, and open resonator antennas for various wireless applications.

Prof. Luk is also a Fellow of the U.K. Royal Academy of Engineering, a Fellow of the Chinese Institute of Electronics, PRC, a Fellow of the Institution of Engineering and Technology, U.K., a Fellow of the Institute of Electrical and Electronics Engineers, USA, and a Fellow of the Electromagnetics Academy, USA. He was awarded ten U.S. and more than ten PRC patents on the design of a wideband patch antenna with an L-shaped probe feed. He received the Japan Microwave Prize, from the 1994 Asia Pacific Microwave Conference held in Chiba, in December 1994, the Best Paper Award from the 2008 International Symposium on Antennas and Propagation held in Taipei, in October 2008, and the Best Paper Award from the 2015 Asia-Pacific Conference on Antennas and Propagation held in Bali, in July 2015. He was awarded the very competitive 2000 Croucher Foundation Senior Research Fellow in Hong Kong. He received the 2011 State Technological Invention Award (Second Honor) of China. He was a recipient of the 2017 IEEE APS John Kraus Antenna Award. He was a Technical Program Chairperson of the 1997 Progress in Electromagnetics Research Symposium (PIERS), a General Vice-Chairperson of the 1997 and 2008 Asia-Pacific Microwave Conference (APMC), a General Chairman of the 2006 IEEE Region Ten Conference (TENCON), a Technical Program Co-Chairperson of 2008 International Symposium on Antennas and Propagation (ISAP), and a General Co-Chairperson of 2011 IEEE International Workshop on Antenna Technology (IWAT), a General Co-Chair of 2014 IEEE International Conference on Antenna Measurements and Applications (CAMA), and a General Co-Chair of 2015 International Conference on Infrared, millimeter, and Terahertz Waves (IRMMW-THz 2015). He is also a General Chair of the 2020 Asia-Pacific Microwave Conference to be held at Hong Kong, in November 2020. He was a Chief Guest Editor for a special issue on ANTENNAS IN WIRELESS COMMUNICATIONS published in the Proceedings of the IEEE, in July 2012. He is also a Deputy Editor-in-Chief of PIERS journals and an Associate Editor of *IET Microwaves and ANTENNAS AND PROPAGATION*.

...